JAM CM Journal of Applied Mathematics and Computational Mechanics 2024, 23(4), 5-17
www.amcm.pcz.pl p-ISSN 2299-9965
DOI: 10.17512/jamcm.2024.4.01 e-ISSN 2353-0588

NUMERICAL TREATMENT BY IMPLEMENTING A SUCCESSIVE APPROXIMATION METHOD FOR FRACTIONAL RICCATI AND LOGISTIC DIFFERENTIAL EQUATIONS

***Mohamed Adel*[1]*, Mohamed M. Khader*[2]**

[1] *Department of Mathematics, Faculty of Science, Islamic University of Madinah Medina, KSA*
[2] *Department of Mathematics and Statistics, College of Science, Imam Mohammad Ibn Saud Islamic University (IMSIU), Riyadh, KSA*
adel@sci.cu.edu.eg, m.adel@iu.edu.sa, mmkhader@imamu.edu.sa

Received: 17 July 2024; Accepted: 16 December 2024

Abstract. The fractional Riccati/Logistic differential equations (FRDE/FLDE) can be accurately solved numerically by using the approach presented in this study. In the provided questions, the fractional derivative is in the Caputo-Fabrizio (CF) sense. The suggested approach is the successive approximation technique (SAM). In this technique, we approximate the solution of the FRDE and FLDE with a finite-dimensional problem. A particular focus is examining the convergence analysis and estimating the upper bound on the error of the obtained approximate scheme. We offer an outcome on worldwide convergence of consecutive estimates. Also, to show the thoroughness of the method proposed, we computed the residual error function. Illustrative instances are given to prove the usefulness and validity of the suggested method.

MSC 2010: *41A10, 65N12, 65N35*
Keywords: *fractional Riccati/logistic differential equation, CF fractional derivative, successive approximations approach, convergence analysis*

1. Introduction

The RDE was named for the Italian ”Jacopo Francesco Riccati” (1676-1744). The basic theories of this equation are presented in Reid’s book [1], which also includes applications to diffusion problems, random processes, and others. Financial mathematics is one of the more recent applications of engineering science, in addition to significant and now traditional applications like network synthesis, optimum control, resilient stabilization, and the stochastic realization theory. Classical numerical techniques like the Runge-Kutta and forward Euler methods can be used to solve this equation. Dubois and Saidi [2] proposed an unconditionally stable method. The nonlinear RDE is solved analytically using the Adomian decomposition method as demonstrated by Bahnasawi et al. [3]. Tan and Abbasbandy [4] used the homotopy analysis approach as an analytical methodology to solve the quadratic Riccati equation. Numerous authors have researched the FDRE, employing various

numerical techniques. To tackle this problem, the variational iteration method is applied, whereas the Adomian decomposition method is used in [5].

The LDE is obtained by solving the logistic equation with the fractional derivative operator. The model was originally published in 1838 by Pierre Verhulst [6, 7]. The population modeling has numerous variables [8]. The Verhulst's model is often used to demonstrate the chaotic behavior and periodic doubling of dynamical systems [7]. According to the model, some factors, such as population density, may be able to restrict population growth [6, 8]. A common use for the logistic curve is in medicine, where tumor growth is modeled using the LDE. This use can be viewed as a continuation of the use described previously within ecology. The explanation for the logistic equation's solution is the population growth rate, which is constant and does not take into account the availability of food or the spread of disease [6]. Let $N(t)$ be the tumor's size at time t and up to the saturation limit, also known as the maximum carrying capacity [6], where $\frac{dN}{dt} = \rho N(1 - \frac{N}{K})$, the model's solution curve increases exponentially. Where N, K, and ρ are the concentrations of the population, carrying capacity, and maximum population growth rate, respectively. A constant growth rate is represented as the solution of the LDE by the formula $N(t) = N_0 e^{\rho t}$, where N_0 represents the starting population [9].

Using a maximum principle, the author [10] demonstrated an abstract monotone iterative system. Numerous publications have been written about the global convergence of the SAM for nonlinear functional differential equations. Using the convergence of consecutive approximations, Browder [11] provided a concise and clear demonstration in 1968 of an expansion on the traditional Picard-Banach contraction theorem [12]. Abbas et al. have recently started the worldwide convergence of consecutive approximations [13, 14]. Several findings on worldwide convergence of sequential approximations for semi-linear differential equations in abstraction can be found in [13], while [14] discusses other findings regarding the Darboux problem for the implicit PDE with successive approximations.

Over the past thirty years, many authors have remained interested in fractional calculus [15]. Researchers have discovered that the creation of innovative fractional derivatives with distinct singular or non-singular kernels is crucial to address the demand for modeling real-world problems in a range of domains, including biology, engineering, and mechanics [16-21]. The CF operator recently proposed a unique operator in the classic Caputo derivative by replacing the singular kernel with the regular kernel [22]. Also, this operator uses a non-singular kernel called the exponential kernel. It can express the memory's whole effect [23]. Numerous issues, including the fractional glioblastoma multiform [24] and the space-time-fractional diffusion equation [25], have seen the effective use of this novel operator.

The primary goal of the research under presentation is to apply the SAM to achieve the numerical solution of the FRED and FLDE, extending earlier work on fractional differential equations. We also give an analysis of the suggested numerical scheme's convergence.

2. Preliminaries

The notation $C := C(\Upsilon, \mathbb{R})$ will be used for the family of continuous functions on the interval $\Upsilon = [0, T]$, which contains all real-valued functions. Let $\psi : \Upsilon \to \mathbb{R}$, associated by the norm [26]:

$$|||\psi(t)||_\infty = \sup_{t\in\Upsilon} |\psi(t)|. \tag{1}$$

$L^1(\Upsilon)$ is the space of all integrable Lebesgue and real-valued measurable functions ψ, furnished with the norm [26]:

$$||\psi(t)||_{L^1} = \int_0^T |\psi(t)|dt. \tag{2}$$

We shall now present the fractional calculus results.

Definition 1 [23] The CF fractional integral ${}^{CF}I^{\nu}$ of order $0 < \nu < 1$ of a function $g(t) \in L^1(\Upsilon)$ is formulated as:

$${}^{CF}I^{\nu} g(t) = \ell(\nu)(1-\nu)g(t) + \nu\,\ell(\nu)\int_0^t g(\tau)d\tau, \tag{3}$$

where $\ell(\nu) = \dfrac{2}{M(\nu)(2-\nu)}$, and $M(\nu)$ is a normalization constant.

Definition 2 [23] The CF fractional derivative ${}^{CF}D^{\nu}$ of order $0 < \nu < 1$ of a function $g(t) \in C(\Upsilon)$ is formulated as:

$${}^{CF}D^{\nu} g(t) = \frac{\ell(\nu)}{(1-\nu)}\int_0^t g^{'}(\tau)\, e^{\frac{-\nu(t-\tau)}{1-\nu}} d\tau, \qquad t \in \Upsilon. \tag{4}$$

For a constant function g, we can see that ${}^{CF}D^{\nu} g(t) = 0$.

Definition 3 [27] The modified CF fractional derivative ${}^{MCF}D^{\nu}$ of order ν of a function $g(t) \in C(\Upsilon)$ is formulated as:

$${}^{MCF}D^{\nu} g(t) = \frac{1}{(1-\nu)}\frac{d}{dt}\int_0^t [g(\tau) - g(0)]\, e^{\frac{-\nu(t-\tau)}{1-\nu}} d\tau, \qquad 0 < \nu < 1. \tag{5}$$

In this definition, for a constant C, we can see that ${}^{MCF}D^{\nu} C = 0$, also as in the original CF fractional-order derivative and the kernel does not have a singularity at $t = \tau$. The MCF fractional-order derivative satisfies the limit conditions [27]:

$$\lim_{\nu\to 1} {}^{MCF}D^{\nu} g(t) = g'(t), \qquad \lim_{\nu\to 0} {}^{MCF}D^{\nu} g(t) = g(t) - g(0). \tag{6}$$

Remark The authors in [30] proved the following formula:

$${}^{CF}I^{\nu}.{}^{CF}D^{\nu} g(t) = g(t) - c, \tag{7}$$

with an arbitrary real constant $c = g(0)$.

Lemma 1 [28] Let $\rho(t) \in L^1([0,T])$. Then the following IVP:

$$ {}^{CF}D^{\nu}\psi(t) = \rho(t), \qquad \psi(0) = \psi_0, \quad t \in [0,T], \tag{8} $$

holds the following unique solution:

$$ \psi(t) = \psi_0 + (1-\nu)\ell(\nu)\left(\rho(t) - \rho(0)\right) + \nu\,\ell(\nu)\int_0^t \rho(\tau)d\tau. \tag{9} $$

3. Basic concepts of the successive approximation method

To show how we can implement the successive approximation method and construct its corresponding numerical scheme, we begin with a general form of the CF fractional IVP:

$$ {}^{CF}D^{\nu}\psi(t) = f(t,\psi(t)), \qquad 0 < \nu < 1, \qquad t \geq 0, \tag{10} $$

with an initial condition $\psi(0) = \psi_0 \in \mathbb{R}$.
Set $\Upsilon_{\varepsilon} := [0, \varepsilon T]$, for any $\varepsilon \in [0,1]$. We are going to state some hypotheses.
(H_1) The function $f : \Upsilon \times \mathbb{R} \to \mathbb{R}$ is continuous.
(H_2) $\exists$ a constant $\gamma > 0$ and a continuous and nondecreasing function $h : \Upsilon \times [0,\gamma] \to \mathbb{R}^+$ and satisfies the following criterion [26]:

$$ |f(t,\psi) - f(t,\bar{\psi})| \leq h(t, |\psi - \bar{\psi}|), \qquad t \in \Upsilon, \quad \psi, \bar{\psi} \in \mathbb{R} \,:\, |\psi - \bar{\psi}| \leq \gamma. \tag{11} $$

(H_3) Let $R \equiv 0$ be a function that belongs to $C(\Upsilon_{\delta}, [0,\gamma])$ and satisfies the criterion:

$$ R(t) \leq \ell(\nu)\left[2(1-\nu)\sup_{(t,\psi)\in\Upsilon_{\delta}\times[0,\gamma]}|f(t,\psi)| + \nu\int_0^{\delta t} h(\tau, R(\tau))d\tau\right], \quad \varepsilon \leq \delta \leq 1. \tag{12} $$

In light of the previous conditions, notes, and Lemma 1, we can define the SA scheme of the model (10) as follows [26]:

$$ \begin{aligned} &\psi_0(t) = \psi_0, \\ &\psi_{n+1}(t) = \psi_0 + \ell(\nu)\left[(1-\nu)\left(f(t,\psi_n(t)) - f(0,\psi_0)\right) + \nu\int_0^t f(\tau,\psi_n(\tau))\,d\tau\right], \\ &n = 0,1,\ldots. \end{aligned} \tag{13} $$

Theorem 1. Suppose the concepts H_i, $i = 1,2,3$ hold. Then the sequence of SAs $\psi_n(t)$, $n = 0,1,\ldots$ which is given in (13); is a uniform convergence to the unique solution of IVP (10) on its domain.

PROOF The proof of this theorem can be found in [26]. ■

4. Numerical implementation

Now, we are going to implement the concepts of the SAM discussed in the previous section to solve numerically each of the FRDE and FLDE.

4.1. Implementation SAM on FRDE

We examine the following form of the FRDE [29]:

$$^{CF}D^{\nu}\psi(t) = 1-\psi^2(t), \qquad \psi(0)=0, \qquad \nu\in(0,1). \tag{14}$$

For $\nu = 1$, Eq. (14) reduces to the standard RDE $\dot{\psi}(t) = 1-\psi^2(t)$ which has the exact solution:

$$\psi(t) = (e^{2t}-1)(e^{2t}+1)^{-1}.$$

To study the existence and uniqueness of the FRDE (14), through the following theorem, we take $\Omega = [0,T]$ and define the space $C(\Omega)$ as the class of all continuous functions defined on Ω, with the norm:

$$||\psi|| = \sup_{t\in\Omega}|e^{-\varepsilon t}\psi(t)|, \quad \varepsilon>0, \tag{15}$$

which is equivalent to the sup-norm $||\psi|| = \sup_{t\in\Omega}|\psi(t)|$.
Also, we define the space:

$$\mathbb{B} = \{\psi\in L_1[0,T], \quad ||\psi|| = ||e^{-\varepsilon t}\psi(t)||_{L_1}\}. \tag{16}$$

Theorem 2 Suppose that the function $\psi(t)$ is bounded, i.e., $|\psi|\leq\kappa$, for some constant κ, also $\psi(t)\in C(\Omega)$, $\psi'(t)\in\mathbb{B}$. Then the initial value problem (14) has a unique solution $\psi(t)$.

PROOF With the help of the properties of fractional calculus (7) [30] and operating with $^{CF}I^{\nu}$, we can rewrite (14) as follows:

$$\psi(t) = c + {}^{CF}I^{\nu}(1-\psi^2(t)), \tag{17}$$

with an arbitrary real constant $c=\psi(0)$. Now, we need to define the operator $\Lambda: C(\Omega)\longrightarrow C(\Omega)$ as follows:

$$\Lambda\psi(t) = {}^{CF}I^{\nu}[1-\psi^2(t)]+c, \tag{18}$$

then

$$\begin{aligned} e^{-\varepsilon t}(\Lambda\psi_1 - \Lambda\psi_2) &= e^{-\varepsilon t}\,{}^{CF}I^{\nu}[(1-\psi_1^2(t)) - (1-\psi_2^2(t))] \\ &\leq \int_0^t \frac{(t-s)^{\nu-1}}{\Gamma(\nu)} e^{-\varepsilon(t-s)}(\psi_1(s)-\psi_2(s))(\psi_1(s)+\psi_2(s))e^{-\varepsilon s}ds \\ &\leq ||\psi_1 - \psi_2|| \int_0^t \frac{s^{\nu-1}e^{-\varepsilon s}}{\Gamma(\nu)}ds, \end{aligned} \tag{19}$$

therefore, we obtain $||\Lambda\psi_1 - \Lambda\psi_2|| \leq ||\psi_1 - \psi_2||$, and this tends to that the operator Λ has a unique fixed point. Consequently, the integral Eq. (17) has a unique solution $\psi \in C(\Omega)$. In addition, it is easy to deduce that ${}^{CF}I^{\nu}(1-\psi^2(t))|_{t=0} = 0$, by connecting the formulas (3) and (14).

The last step in the proof is to prove the equivalence between the integral equation (17) and the initial value problem (14) as follows:

From Eq. (17) and use ${}^{CF}I^{\nu} = {}^{CF}I^{\nu}I\frac{d}{dt}$, we can formally have:

$$\psi(t) = \Big[c + {}^{CF}I^{\nu+1}(0 - 2\psi(t)\psi'(t))\Big],$$

$$\frac{d\psi}{dt} = \Big[{}^{CF}I^{\nu}(-2\psi(t)\psi'(t))\Big],$$

$$e^{-\varepsilon t}\psi'(t) = e^{-\varepsilon t}\Big[{}^{CF}I^{\nu}(-2\psi(t)\psi'(t))\Big],$$

from which we can conclude that $\psi \in C(\Omega)$ and $\psi' \in \mathbb{B}$. Now, from Eq. (17), we get

$$\frac{d\psi}{dt} = \frac{d}{dt}\,{}^{CF}I^{\nu}[1-\psi^2(t)],$$

$${}^{CF}I^{1-\nu}\frac{d\psi}{dt} = {}^{CF}I^{1-\nu}\frac{d}{dt}\,{}^{CF}I^{\nu}[1-\psi^2(t)] = \frac{d}{dt}\,{}^{CF}I^{1-\nu}\,{}^{CF}I^{\nu}[1-\psi^2(t)],$$

$${}^{CF}D^{\nu}\psi(t) = \frac{d}{dt}I[1-\psi^2(t)] = 1-\psi^2(t), \text{ and } \psi(0) = 0,$$

this means that the integral equation (17) is equivalent to the IVP (14), and the theorem is proved. ∎

According to the successive approximation (13), we can construct a numerical scheme of the problem (14) in the interval $\Upsilon = [0, 2.5]$ as follows:

$$\psi_0(t) = 0, \quad t \in \Upsilon,$$
$$\psi_{n+1}(t) = \left(\frac{2}{(2-\nu)M(\nu)}\right)\left[(1-\nu)\left(\mathbb{F}(t,\psi_{\mathrm{n}}(t)) - \mathbb{F}(0,0)\right) + \nu\int_0^t \mathbb{F}(\tau,\psi_n(\tau))\,d\tau\right]. \tag{20}$$

This SA form is convergent uniformly on its domain according to Theorem 1 to the unique solution of (14). Here $\mathbb{F}(t,\psi(t)) = 1-\psi^2(t)$.

Here, to present a complete numerical study with simulation, we consider and define the residual error function (REF) [31] as follows:

$$\mathrm{REF}(t,\nu,n) = {}^{CF}D^{\nu}\psi_n(t) + \psi_n^2(t) - 1. \tag{21}$$

Table 1. A comparison of the REF from solving the FRDE at various values of n at $\nu = 0.9$

t	$n=10$	$n=15$	$n=20$	$n=25$	$n=30$
0.0	4.6542E-3	1.0074E-4	9.9514E-5	2.6540E-6	3.7530E-7
0.5	4.7520E-3	5.0147E-4	6.9520E-5	7.7589E-5	0.3021E-6
1.0	1.4452E-2	3.7530E-3	0.8501E-5	9.5421E-6	2.9328E-7
1.5	3.1597E-2	4.4568E-3	8.7419E-4	3.1204E-6	4.9317E-7
2.0	1.6541E-3	3.0147E-4	4.7204E-5	5.6514E-5	0.9017E-6
2.5	1.0258E-2	0.2580E-3	6.7536E-4	4.5621E-6	3.9755E-7

In all cases, the smallness of the residual ($\mathrm{REF}(t,\nu,n) \to 0$) means that the approximate solution is close to the exact solution, i.e., the absolute relative error tends to be zero. We used this type of error because the exact solution is unknown in the case of ν, which is a fractional value. Finally, to achieve this aim and validate our numerical solutions, we compute the REF with different values of n,t, at $\nu = 0.9$ through Table 1. The results included in this table show the thoroughness of the method proposed in this article, and that the error can be controlled and reduced with increasing n.

Figures 1 through 3 display the numerical results of the model (14) in the interval $[0,2.5]$, with varying initial solutions $\hat{\psi}$ and fractional order ν values; also, the number of iterations n of the numerical scheme (20) varies. $M(\nu) = \dfrac{2}{2-\nu}$ is what we use.

1. Figure 1 shows a comparison between the exact solution ($\nu = 1$) and numerical solution (with $n = 15$) utilizing the previously introduced technique.
2. Figure 2 examines the behavior of the numerical solution with $\hat{\psi} = 0.0$ and $n = 20$, using various values of $\nu = 0.95, 0.85, 0.75, 0.65$.
3. Figure 3 gives the behavior of the numerical solution with various initial solutions $\hat{\psi} = 0.2, 0.4,\ 0.6, 0.8$, at $\nu = 0.9$ and $n = 25$.

These figures allow us to conclude that the approach can be used to solve the given problem because the behavior of the obtained numerical solution is in excellent agreement with the exact solution.

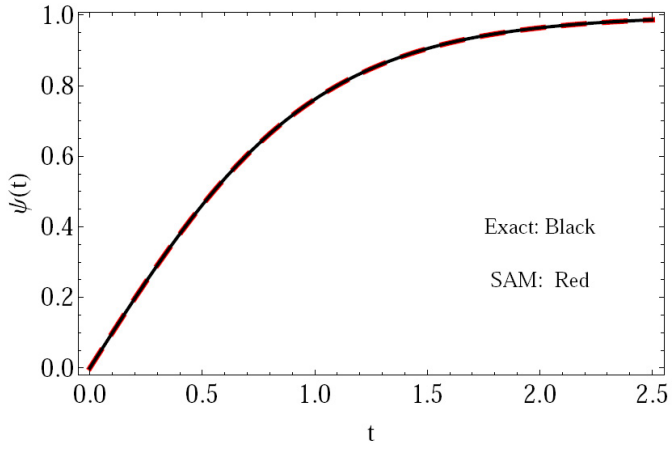

Fig. 1. A comparison between the exact solution and numerical solution of the FRDE using SAM at $\nu = 1$

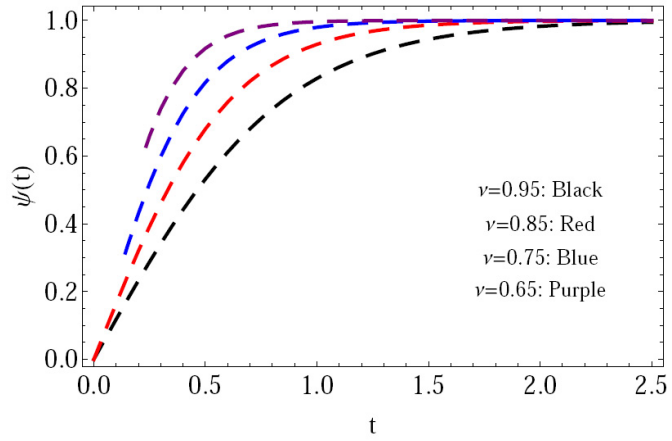

Fig. 2. The numerical solution of the FRDE with different values of ν at $\hat{\psi} = 0.0$

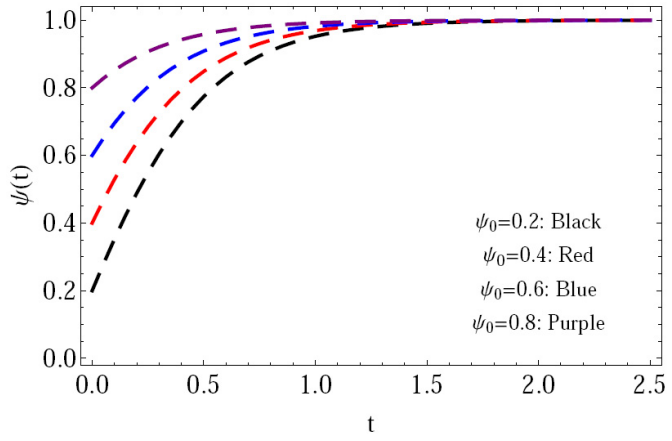

Fig. 3. The numerical solution of the FRDE with different initial solutions $\hat{\psi}$ at $\nu = 0.9$

4.2. Implementation of SAM on FLDE

In this example, we consider the following FLDE [32]:

$$ {}^{CF}D^{\nu}\theta(t) = \beta\theta(t)(1-\theta(t)), \qquad \theta(0) = \hat{\theta}, \qquad \beta > 0. \tag{22} $$

For $\nu = 1$, Eq. (22) reduces to the standard LDE $\dot{\theta}(t) = \beta\theta(t)(1-\theta(t))$, with the exact solution $\theta(t) = \hat{\theta}\left((1-\hat{\theta})e^{-\beta t} + \hat{\theta}\right)^{-1}$.
The existence and uniqueness of (22) can be found in detail [32].

According to the successive approximation (13), we can construct a numerical scheme of the model (22) in $\Upsilon = [0,1]$ as follows:

$$ \theta_0(t) = \hat{\theta}, \quad t \in \Upsilon, $$
$$ \theta_{n+1}(t) = \hat{\theta} + \left(\frac{2}{(2-\nu)M(\nu)}\right)\left[(1-\nu)\left(\mathbb{G}(t,\theta_{\mathrm{n}}(t)) - \mathbb{G}(0,\hat{\theta})\right) + \nu\int_0^t \mathbb{G}(\tau,\theta_n(\tau))\,d\tau\right]. \tag{23} $$

Here $\mathbb{G}(t,\theta(t)) = \beta\theta(t)(1-\theta(t))$.
To present a complete numerical study with simulation, we consider the REF as follows:

$$ \mathrm{REF}(t,\nu,n) = {}^{CF}D^{\nu}\theta_n(t) - \beta\,\theta_n(t)(1-\theta_n(t)). \tag{24} $$

To achieve this aim and validate our numerical solutions, we compute the REF with different values of n,t, at $\nu = 0.9$ through Table 2. The results included in this table show the thoroughness of the method proposed in this article, and that the error can be controlled and reduced with increasing n.

Table 2. A comparison of the REF from solving the FLDE at various values of n at $\nu = 0.9$

t	$n=10$	$n=15$	$n=20$	$n=25$	$n=30$
0.0	2.5387E-2	3.3201E-3	2.6214E-4	0.0147E-5	7.9217E-7
0.2	6.7536E-2	1.4521E-3	0.3214E-4	4.0159E-5	6.7536E-6
0.4	6.7536E-2	2.9521E-3	4.4521E-4	2.7410E-5	0.9632E-7
0.6	1.9214E-2	4.6541E-3	3.7530E-4	2.0214E-5	7.3201E-7
0.8	5.7536E-2	1.1230E-3	6.7504E-4	3.0054E-5	1.9541E-7
1.0	1.3258E-2	3.7521E-3	4.4520E-4	7.7524E-5	2.6627E-6

The numerical results of the given model (22) in the interval $[0,1]$ are given in Figures 4 to 6 with various values of the fractional order ν, and initial solutions $\hat{\theta}$; with different numbers of iterations n of the numerical scheme (23). We take $M(\nu) = \dfrac{2}{2-\nu}$.

1. Figure 4 gives a comparison between the exact solution $\nu = 1$, and the numerical solution at $\hat{\theta} = 0.25$, $n = 15$ using the proposed numerical scheme.

2. Figure 5 presents the numerical solution with different values of $\nu = 0.95, 0.85, 0.75, 0.65$ at $\hat{\theta} = 0.25$ and $n = 20$.

3. Figure 6 shows the effect of the parameter β on the behavior of the numerical solution with different values of $\beta = 0.3, 0.6, 0.9, 1.2$ at $\nu = 0.9$, $\hat{\theta} = 0.1$, and $n = 25$.

These figures allow us to conclude that the approach can be used to solve the given problem because the behavior of the obtained numerical solution is in excellent agreement with the exact solution. In addition, the obtained numerical solutions depend on the changes in the values of parameters $\nu, n, \hat{\theta}$, and β.

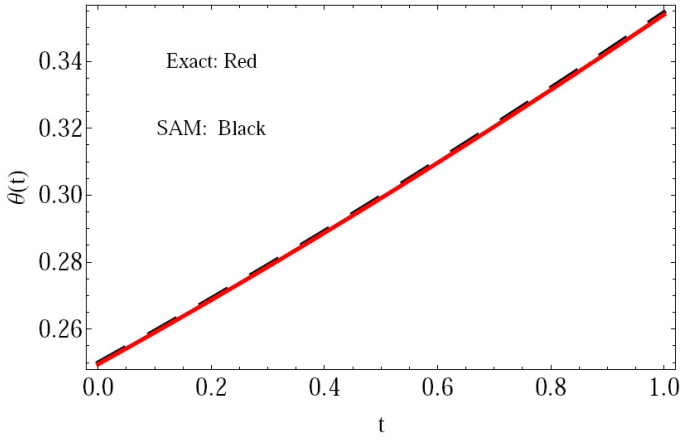

Fig. 4. A comparison between the exact solution and numerical solution of the FLDE using SAM at $\nu = 1$

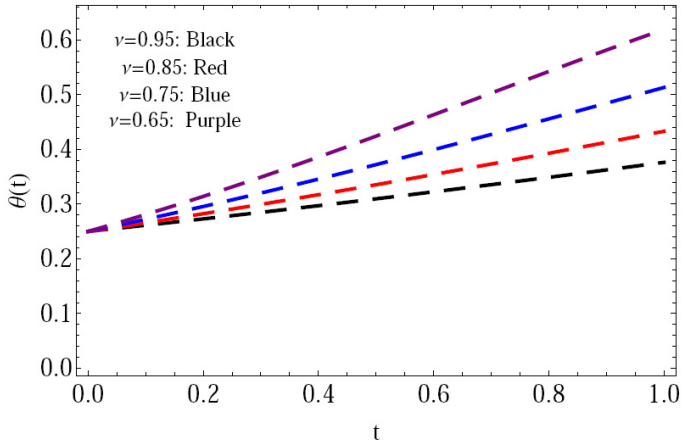

Fig. 5. The numerical solution of the FLDE with different values of ν at $\hat{\theta} = 0.25$

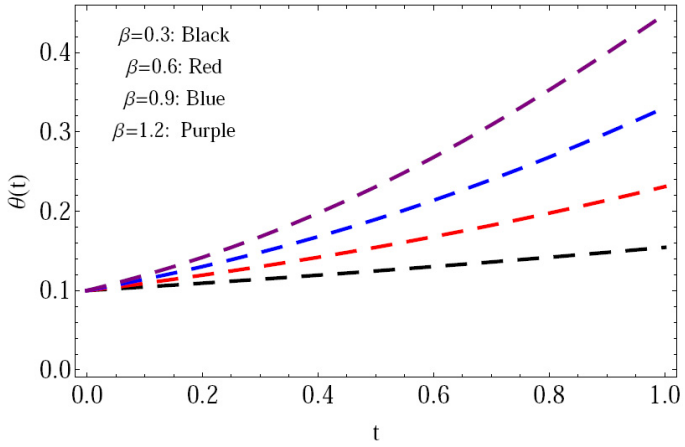

Fig. 6. The approximate solution of the FLDE with different values of β

5. Conclusions

The goal of this research is to apply the successive approximation method to the numerical investigation of two popular models: the FRDE and FLDE. We offer a numerical simulation of the two suggested problems, with varying initial solutions and fractional order values ν; we also vary the number of iterations n of the proposed numerical schemes. Also, in each of the two proposed models, we compared the obtained numerical solutions and the exact solution at $\nu = 1$. This comparison allows us to conclude that the numerical solution achieved by applying the suggested scheme is in excellent agreement with the exact solution. It also demonstrates the effectiveness of this approach in solving the problems and highlights the validity and enormous potential of the offered strategy. Furthermore, the derived scheme's error upper bound is inferred. The sequence of the obtained numerical solution converges as the number of iterations, n, increases, according to the numerical results. This paper was computed entirely in Mathematica 8.0. Finally, it is vital to look into analytical and numerical solutions for FDEs because they have recently become models in various areas of applied mathematics.

Acknowledgments

The researchers wish to extend their sincere gratitude to the Deanship of Scientific Research at the Islamic University of Madinah for the support provided to the Post-Publishing Program.

References

[1] Reid, W.T. (1972). *Riccati Differential Equations, Mathematics in Science and Engineering*. New York: Academic Press, 86.

[2] Dubois, F., & Saidi, A. (2000). Unconditionally stable scheme for Riccati equation. *ESAIM Proceedings*, *8*, 39-52.

[3] Bahnasawi, A.A., El-Tawil, M.A., & Abdel-Naby, A. (2004). Solving Riccati differential equation using ADM. *Appl. Math. Comput.*, *157*, 503-514.

[4] Tan, Y., & Abbasbandy, S. (2008). Homotopy analysis method for quadratic Riccati differential equation. *Commun. Nonlin. Sci. Numer. Simul.*, *13*(3), 539-546.

[5] Momani, S., & Shawagfeh, N. (2006). Decomposition method for solving fractional Riccati differential equations. *App. Mathem. Comput.*, *182*, 1083-1092.

[6] Pastijn, H. (2006). *Chaotic Growth with the Logistic Model of P.-F. Verhulst, Understanding Complex Systems*. In: *The Logistic Map and the Route to Chaos: From the Beginnings to Modern Applications*. Berlin-Heidelberg: Springer-Verlag.

[7] Alligood, K.T., Sauer, T.D., & Yorke, J.A. (1996). An Introduction to Dynamical Systems. *Springer*.

[8] Ausloos, M., & Dirickx (eds.) (2006). *The Logistic Map and the Route to Chaos: From the Beginnings to Modern Applications*. Berlin-Heidelberg: Springer-Verlag.

[9] Suansook, Y., & Paithoonwattanakij, K. (2009). Dynamic of logistic model at fractional order. *IEEE International Symposium on Industrial Electronics*.

[10] Nieto, J.J. (1997). An abstract monotone iterative technique. *Nonlinear Anal., Theory, Methods and Appl.*, *28*, 1923-1933.

[11] Browder, F. (1968). On the convergence of successive approximations for nonlinear functional equations. *Indag. Math.*, *30*, 27-35.

[12] Człapiński, T. (2014). Global convergence of successive approximations of the Darboux problem for partial functional differential equations with infinite delay. *Opuscula Math.*, *34*(2), 327-338.

[13] Abbas, S.A., & Benchoro, A.M. (2019). Global convergence of successive approximations for abstract semilinear differential equations. *Pan. Amer. Math. J.*, *29*(3), 17-31.

[14] Abbas, S.A., Benchoro, A.M., & Hmiddt, N. (2018). Successive approximations for the Darboux problem for implicit partial differential equations. *Pan. Amer. Math. J.*, *28*(3), 1-10.

[15] Adel, M., Khader, M.M., & Algelany, S. (2023). High-dimensional chaotic Lorenz system: Numerical treated using Changhee polynomials of the Appell type. *Fractal and Fractional*, *7*(5), 1-16.

[16] Adel, M., Sweilam, N.H., Khader, M.M., Ahmed, S.M., Ahmad, H., & Botmart, T. (2022). Numerical simulation using the non-standard weighted average FDM for 2Dim variable-order Cable equation. *Results in Physics*, *39*, 105682.

[17] Alkathiri, A.A., Jamshed, W., Devi, S.U.S., Eid, M.R., & Bouazizi, M.L. (2022). Galerkin finite element inspection of the thermal distribution of renewable solar energy in the presence of binary nanofluid in parabolic trough solar collector. *Alexandria Engineering Journal*, *61*, 11063-11076.

[18] Ouni, M., Ladhar, L.M., Omri, M., & Jamshed W. (2022). Solar water-pump thermal analysis utilizing copper?gold/engine oil hybrid nanofluid flowing in parabolic trough solar collector: Thermal case study. *Case Studies in Thermal Engineering*, *30*, 101756.

[19] Jamshed, W., Shahzad, F., Safdar, R., Sajid, T., Eid, M.R., & Nisar, K.S. (2024). Implementing renewable solar energy in the presence of Maxwell nanofluid in parabolic trough solar collector: a computational study. *Waves in Random and Complex Media*, *34*(5), 4320-4351.

[20] Jamsheda, W., Devi, S.U.S., Safdar, R., Redouaned, F., Nisare, K.S., & Eid, M.R. (2021). Comprehensive analysis on copper-iron (II, III)/oxide-engine oil Casson nanofluid flowing and thermal features in parabolic trough solar collector. *Journal of Taibah University for Science*, *15*(1), 619-636.

[21] Jamshed, W., Eid, M.R., Nasir, N.A.A.M., Nisar, K.S., Aziz, A., Shahzad, F., Saleel, A., & Shukla, A. (2021). Thermal examination of renewable solar energy in parabolic trough solar collector utilizing Maxwell nanofluid: A noble case study. *Case Studies in Thermal Engineering*, *27*, 101258.

[22] Abdulhameed, M., Vieru, D., & Roslan, R. (2017). Magnetohydrodynamic electroosmotic flow of Maxwell fluids with Caputo-Fabrizio derivatives through circular tubes. *Computers & Mathematics with Applications*, *74*(10), 2503-2519.

[23] Caputo, M., & Fabrizio, A. (2015). A new definition of fractional derivative without singular kernel. *Progress in Fractional Differentiation and Applications*, *1*(2), 73-85.

[24] Mahdy, A.M.S. (2023). Stability, existence, and uniqueness for solving fractional glioblastoma multiforme using a Caputo-Fabrizio derivative. *Mathematical Methods in the Applied Science*, *15*, 1-18.

[25] Aguilar, J.G. (2017). Space-time fractional diffusion equation using a derivative with nonsingular and regular kernel. *Physica A: Statistical Mechanics and its Applications*, *465*, 562-572.

[26] Bachir, F.S., Abbas, S., Benbachir, M., & Benchohra, M. (2022). Successive approximations for Caputo-Fabrizio fractional differential equations. *Tatra Mountains Mathematical Publications*, *81*, 1, 117-128.

[27] Martinez, H.Y., & Gomez-Aguilar, J.F. (2019). A new modified definition of Caputo--Fabrizio fractional-order derivatives and their applications to the multi-step homotopy analysis method. *Journal of Computational and Applied Mathematics*, *346*, 247-260.

[28] Shaikh, A., Tassaddiq, A.S., Nisar, K., & Baleanu, D. (2019). Analysis of differential equations involving the Caputo-Fabrizio fractional operator and its applications to reaction-diffusion equations. *Adv. Difference Equ.*, *178*, 1-14.

[29] Khader, M.M., Sweilam, N.H., & Kharrat, B.N. (2020). Numerical simulation for solving fractional Riccati and Logistic differential equations as a difference equation. *Applications and Applied Mathematics: An Inter. Journal*, *15*(1), 655-665.

[30] Losada J., & Nieto, J.J. (2021). Fractional integral associated to fractional derivatives with nonsingular kernels. *Progr. Fract. Differ. Appl.*, *7*(3), 137-143.

[31] Parand, K., & Delkhosh, M. (2016). Operational matrices to solve nonlinear Volterra--Fredholm IDEs of multi-arbitrary order. *Gazi University J. of Science*, *29*(4), 895-907.

[32] El-Sayed, A.M.A., El-Mesiry, A.E.M., & El-Saka, H.A.A. (2007). On the fractional--order Logistic equation. *Applied Mathematics Letters*, *20*(7), 817-823.